Non-cyanobacterial diazotrophs dominate dinitrogen fixation in biological soil crusts at the early stage of crust formation.

Charles Pepe-Ranney [1], **Chantal Koechli** [1], **Ruth Potrafka** [2], **Ferran Garcia-Pichel** [2], **Daniel H Buckley** [1,*]

[1] *Cornell University, Department of Crop and Soil Sciences, Ithaca, NY, USA*
[2] *Arizona State University, School of Life Sciences, Tempe, AZ 85287, USA.*

Correspondence*:
Daniel H Buckley
Cornell University, Department of Crop and Soil Sciences, Ithaca, NY, USA,

1 ABSTRACT

Biological soil crusts (BSC) cover a vast global area and are key components of ecosystem productivity in arid soils. In particular, BSC contribute significantly to the nitrogen (N) budget via N_2-fixation. N_2-fixation in mature crusts is largely attributed to heterocystous cyanobacteria, however, early successional crusts possess few N-fixing cyanobacteria and this suggests that microorganisms other than cyanobacteria mediate N_2-fixation during the early stages of BSC development. DNA stable isotope probing (DNA-SIP) with $^{15}N_2$ revealed that *Clostridiaceae* and *Proteobacteria* are the most common microorganisms to assimilate ^{15}N in early successional crusts. The maximum $^{15}N_2$-assimilating *Clostridiaceae* and *Proteobacteria* Operational Taxonomic Unit (OTU, all sequences at least 97% sequence identity to OTU seed) relative abundance in environmental BSC SSU rRNA gene sequence surveys was 0.00225% and 0.00127% in any single sample, respectively. Their low abundance may explain why these heterotrophic diazotrophs have not previously been characterized in BSC. Diazotrophs play a critical role in BSC formation and characterization of these organisms represents a crucial step towards understanding how antropogenic change will effect the formation and ecological function of BSC in arid ecosystems.

2 INTRODUCTION

Biological soil crusts (BSC) are specialized microbial mat communitites that form at the soil surface in arid environments and fill a variety of important ecological functions. BSC occupy plant interspaces and cover a wide, global geographic range (Garcia-Pichel et al., 2003b). The ground cover of BSC on the Colorado Plateau has been measured as high as 80% by remote sensing (Karnieli et al., 2003). The global biomass of BSC *Cyanobacteria* alone is estimated at 54 x 10^{12} g C (Garcia-Pichel et al., 2003b). BSC are responsible for significant nitrogen (N) flux (for review of BSC N_2-fixation see Belnap (2003)). N_2-fixation represents the dominant source of new ecosystem N in more than 80% of BSC from diverse sites across North America, Africa, and Australia (Evans and Belnap, 1999), while atmospheric N deposition was a dominant source of N in only a minority of sites. The presence of BSC is positively correlated with vascular plant survival due in part to BSC ecosystem N contributions (for review of BSC-vascular plant interactions see Belnap et al. (2003)). Climate change and disturbance could alter BSC microbial community structure/membership and possibly BSC diazotroph diversity and N_2-fixation.

BSC N_2-fixation rate studies (typically employing the acetylene reduction assay (ARA)) have explored BSC diazotroph activity across various ecological gradients. Reported BSC N_2-fixation rates vary

29   significantly across samples and studies (Evans and Lange, 2001). The reasons for inter-site and inter-
30   study variability are complex and likely include the spatial heterogeneity of BSC (Evans and Lange,
31   2001) and the impact of recent environmental change on N_2-fixation rates (see Belnap (2001) for
32   discussion). Moreover, the ARA assay is subject to methodological artifacts that can complicate making
33   robust comparisons across sample types that differ in physical and biological characteristics (see Belnap
34   (2001) for review). Nonetheless, N_2-fixation rates are consistently higher in mature BSC than in early
35   successional BSC (Belnap, 2002; Yeager et al., 2004). This difference may be due to the proliferation
36   of heterocystous *Cyanobacteria* in mature BSC and is consistent with the theory that heterocystous
37   *Cyanobacteria* provide the main source of fixed-N. Alternatively, the N_2-fixation rate differences between
38   early successional and mature BSC might be attributable to methodological artifacts. For instance, N_2-
39   fixation in mature BSC is maximal at the crust surface (coincident with heterocystous cyanobacteria)
40   while it is maximal below the crust surface in early successional BSC (Johnson et al., 2005). Diffusional
41   limitation can cause ARA to underestimate N_2-fixation which occurs below the crust surface and as a
42   result ARA can systematically underestimate rates of N_2-fixation in early successional BSC (Johnson
43   et al., 2005). Diffusion would not be an issue when measuring N_2-fixation rates in mature crusts as
44   nitrogenase activity peaks near the surface. The difference between N_2 fixation rates of early successional
45   and mature BSC were not statistically significant when total rates were estimated by integrating multiple
46   rates from thin (1-3mm) slices along BSC depth profiles (as opposed to intact cores) (Johnson et al., 2005).

47   Molecular studies of BSC microbial diversity include explorations of the BSC microbial community
48   vertical profile (Garcia-Pichel et al., 2003a), BSC *nifH* gene content surveys (e.g. Yeager et al. (2004),
49   Yeager et al. (2012), Yeager et al. (2006) and Steppe et al. (1996)), and next-generation-sequencing (NGS)
50   enabled studies of BSC SSU rRNA genes across wide geographic ranges (Garcia-Pichel et al., 2013;
51   Steven et al., 2013). Early successional BSC are often described as "light" in appearance relative to "dark"
52   mature BSC (Belnap, 2002; Yeager et al., 2004). Mature BSC possess greater numbers of heterocystous
53   *Cyanobacteria* (i.e *Scytonema*, *Spirirestis*, and *Nostoc* (Yeager et al., 2006, 2012)) than developing
54   BSC but both early successional and mature BSC are dominated by non-heterocystous *Cyanobacteria*
55   (*Microcoleus vaginatus* or *M. steenstrupii*) (Yeager et al., 2004; Garcia-Pichel et al., 2013). Heterocystous
56   *Cyanobacteria* are the numerically dominant BSC diazotrophs in *nifH* clone libraries (Yeager et al., 2006,
57   2004, 2012). Eighty-nine perent of 693 *nifH* sequences derived from Colorado Plateau and New Mexico
58   BSC samples were described as heterocystous cyanobacterial (non-cyanobacterial *nifH* sequences were
59   largely attributed to alpha- and beta- *Proteobacteria*) (Yeager et al., 2006). However, an early survey of
60   Colorado Plateau BSC *nifH* diversity recovered *nifH* genes related to *Gammaproteobacteria* as well as
61   a clade that included *nifH* genes from the anaerobes *Clostridium pssteurianum*, *Desulfovibrio gigas* and
62   *Chromatium buderi*,

63   The influence of microbial community membership and structure on BSC N_2-fixation is an ongoing
64   research question (Belnap, 2013). While the presence/abundance of heterocystous *Cyanobacteria* has
65   been proposed as the mechanism behind increased N_2-fixation in mature BSC, it is unclear if mature BSC
66   actually fix more N than early successional BSC (see Johnson et al. (2005)). More studies are necessary
67   to elucidate the microbial membership influence on BSC N_2-fixation and to determine if heterocystous
68   *Cyanobacteria* are the only keystone diazotrophs. The first step in defining structure function relationships
69   with respect to N_2-fixation is a full accounting of BSC diazotrophs. Towards this end we conducted
70   $^{15}N_2$ DNA stable isotope probing (DNA-SIP) experiments with early successional Colorado Plateau BSC.
71   DNA-SIP with $^{15}N_2$ has not been previously attempted with BSC. DNA-SIP provides an accounting
72   of *active* diazotrophs whereas *nifH* clone libraries account for microbes with the genomic potential for
73   N_2-fixation. Further, we investiage the distribution of these active diazotrophs in BSC NGS microbial
74   diversity surveys over a range of spatial scales and soil types (Garcia-Pichel et al., 2013; Steven et al.,
75   2013).

3 RESULTS

3.1 ORDINATION OF CSCL GRADIENT FRACTION SSU RRNA SEQUENCE COLLECTIONS SHOWS HEAVY FRACTIONS FROM CONTROL AND LABELED CSCL GRADIENTS ARE DIFFERENT

76 BSC were incubated for 4 days in the presence or absence of $^{15}N_2$ and DNA was extracted for DNA-SIP
77 at 2 and 4 days. Fractionation of CsCl gradients permitted separation of DNA on the basis of buoyant
78 density. Ordination of Bray-Curtis (Bray and Curtis, 1957) distances between gradient fractions (based on
79 OTU abundance within each fraction) reveals that labeled gradient fractions (i.e. gradient fractions from
80 CsCl gradients with $^{15}N_2$ labeled DNA) diverge from control (i.e. DNA from incubations without $^{15}N_2$)
81 at the heavy end of the CsCl gradients (Figure 1 and Figure S1). Bray-Curtis distances between heavy
82 gradient fractions are consistent label/control groups (p-value: 0.001, r^2: 0.18, Adonis test (Anderson,
83 2001)).

3.2 OTUS RESPONSIVE TO $^{15}N_2$ ARE PRIMARILY *PROTEOBACTERIA* AND *CLOSTRIDIACEAE*

84 A statistically significant increase in OTU abundance in heavy fractions of $^{15}N_2$ labeled samples relative
85 to corresponding control fractions provides evidence for OTUs that have incorporated ^{15}N into their DNA.
86 Specifically, we compared OTU proportion means between labeled and control samples from heavy
87 gradient fractions using statistics developed to find differentially expressed genes with RNASeq data
88 (McMurdie and Holmes, 2014; Love et al., 2014). OTUs that incorporated ^{15}N into DNA and increased
89 in bouyant density were identified by rejecting the the null hypothesis that the labeled versus control
90 proportion mean ratio for an OTU (considering only heavy fractions) was below a chosen threshold (see
91 methods). p-values were adjusted by the BH method (Benjamini and Hochberg, 1995) and we used a
92 false discovery rate (FDR) cutoff of 0.10 (typical FDR threshold in gene expression data analysis). A total
93 of 2,127 and 2,160 OTUs were detected in days 2 and 4, respectively, and interrogated for evidence of
94 $^{15}N_2$-labelling. Of these OTUs, only 208 and 233, respectively, passed a sparsity threshold we applied as
95 an independent filtering step to pre-screen out OTUs not likely to produce significant p-values (see Love
96 et al. (2014) for discussion of independent filtering). Of OTUs passing sparsity criteria 38 were found to be
97 enriched significantly in heavy fractions relative to control. These OTUs likely incorporated ^{15}N into DNA
98 ($^{15}N_2$ "responders"). Of these 38, 26 are annotated as *Firmicutes*, 9 as *Proteobacteria*, 2 as *Acidobacteria*
99 and 1 as *Actinobacteria* (Figure 3, Figure 2). If the responder OTUs are ranked by descending, moderated
100 proportion mean labeled:control ratios, the top 10 ratios (i.e. the 10 OTUs that were most enriched in the
101 labeled gradients considering only heavy fractions) are either *Firmicutes* (6 OTUs) or *Proteobacteria* (4
102 OTUs) (Figure 4). Centroid or seed sequences for strongly responding *Proteobacteria* OTUs all share high
103 sequence identity (>98.48%, Table 1) with cultivars from genera known to possess diazotrophs including
104 *Klebsiella*, *Shigella*, *Acinetobacter*, and *Ideonella*. None of the *Firmicutes* OTU centroids in the top 10
105 responders share greater than 97% sequence identity with sequences in the LTP database (release 115)
106 (see Table 1). OTUs that passed the sparsity threshold but were not classified as ^{15}N-responsive were
107 subsequently tested with the null hypothesis that the OTU proportion mean ratio was above the selected
108 threshold. Rejecting the second null would indicate an OTU did *not* incorporate ^{15}N into biomass. There
109 were 58 and 70 "non-responders" at days 2 and 4, respectively. OTUs that did not pass sparsity or could not
110 be classified as either a responder or non-responder are simply ambiguous with respect to ^{15}N labelling.

3.3 ^{15}N-RESPONSIVE OTUS IN ENVIRONMENTAL SAMPLES

111 Five of the 6 *Firmicutes* with the strongest response to ^{15}N-labelling (Table 1) belong in the *Clostridiacea*.
112 We only observed one of these strongly responding *Clostridiaceae* in the data presented by Garcia-Pichel
113 et al. (2013), "OTU.108" (closest BLAST hit in LTP Release 115 – *Caloramotor proteoclasticus*, BLAST

114 %ID 96.94, Accession X90488). OTU.108 was found in two samples both characterized as "light" (i.e.
115 early successional) crust. One other *Clostridiaceae* OTU with a proportion mean ratio (labeled:control)
116 p-value less than 0.10 but outside the top 10 responders was found in the Garcia-Pichel et al. (2013)
117 data (a "light" crust sample) (Figure 2). None of the strongly responding *Clostridiacea* were found in the
118 sequences in Steven et al. (2013) (Figure 2). *Clostridiaceae* ^{15}N-responder OTUs are not closely related to
119 cultivars. (Table 1, Figure 5). One of the proteobacterial OTUs with the strongest ^{15}N response (Table 1)
120 was found in Garcia-Pichel et al. (2013) samples (closest BLAST hit in LTP Release 115, BLAST
121 %ID 100, Accession ZD3440, *Acinetobacter johnsonii*). None of the strongly responding *Protebacteria*
122 OTUs were found in the Steven et al. (2013) samples. A responder OTU was found in a Steven et al.
123 (2013) sample 133 times. Eighty-three times in sub-biocrust samples, 50 times in crust samples (see
124 Figure 2). Two ^{15}N-responsive OTUs were found in an extensive number of environmental samples (61
125 of 65 samples from the combined data sets of Garcia-Pichel et al. (2013) and Steven et al. (2013)). Both
126 OTUs were annotated as *Acidobacteria* but shared little sequence identity to any cultivar SSU rRNA
127 gene sequences in the LTP (Release 115), with best LTP BLAST hits of 81.91 and 81.32% identity
128 (Table 1). Additionally, the magnitude of the ^{15}N-response for each OTU was weak relative to other
129 putative responders (3. Of the remaining 36 stable isotope responder OTUs, only 14 were observed in the
130 environmental data (Figure 2, Figure S5).

3.4 COMPARING SEQUENCE COLLECTIONS AT "STUDY"-LEVEL

131 We compared the sequences this DNA-SIP experiment to two previous surveys of SSU rRNA amplicons
132 from BSC communities: the Garcia-Pichel et al. (2013) and Steven et al. (2013) study. There were 3,079
133 OTUs (209,354 total sequences after quality control) in the DNA-SIP data, 3,203 OTUs (129,033 total
134 sequences after quality control) in the Garcia-Pichel et al. (2013) study, and 2,481 OTUs (129,358 total
135 sequences after quality control) in the Steven et al. (2013) study. There were a total of 4,340 OTUs
136 in all three datasets. Of the total 4,340 OTU centroids established for this study, 445 have matches in
137 the Living Tree Project (LTP) (a collection of 16S gene sequences for all sequenced type strains (Yarza
138 et al., 2008)) at greater or equal than 97% sequence identity (LTP version 115). That is, 445 of 4,340
139 OTUs are closely related to cultivars. The DNA-SIP data set shares 56% OTUs with the Steven et al.
140 (2013) data and 46% of OTUs with the Garcia-Pichel et al. (2013) data (where total OTUs are from
141 the combined data for each pairwise comparison). The Steven et al. (2013) and Garcia-Pichel et al.
142 (2013) studies share 46% of OTUs. *Cyanobacteria* and *Proteobacteria* were the top two phylum-level
143 sequence annotations for all three studies of BSC. Only the DNA-SIP data had more *Proteobacteria*
144 annotations than *Cyanobacteria*. *Proteobacteria* represented the 29.8% of sequence annotations in DNA-
145 SIP data as opposed to 17.8% and 19.2% for the Garcia-Pichel et al. (2013) and Steven et al. (2013) data,
146 respectively. There is a contrast in the total percentage of sequences annotated as *Firmicutes* between the
147 raw environmental samples and the DNA-SIP data. *Firmicutes* represent only 0.21% and 0.23% of total
148 phylum level sequence annotations in the Steven et al. (2013) and Garcia-Pichel et al. (2013) studies,
149 respectively (Figure S2). In the DNA-SIP sequence collection *Firmicutes* make up 19% of phylum level
150 sequence annotations. SIP places focus upon organisms based on isotope incorporation and has the ability
151 to detect activity by low abundance members of the community. DNA from OTUs that incopororate [15]N
152 into their biomass moves towards the heavy end of the CsCl gradient and therefore OTUs in "labeled"
153 DNA are enriched in the full data pool relative to bulk DNA. Phylum-level taxonomic annotations of
154 ^{15}N-responsive OTUs (i.e. *Firmicutes* and *Proteobacteria*) are enriched in the DNA-SIP data relative
155 to environmental data (Figure S2). Also in contrast for the DNA-SIP versus environmental data is the
156 number of putative heterocystous *Cyanobacteria* sequences. Only 0.29% of *Cyanobacteria* sequences in
157 the DNA-SIP data are annotated as belonging to "Subsection IV" which is the heterocystous order of
158 *Cyanobacteria* in the Silva taxonomic nomenclature (Pruesse et al., 2007). In the Steven et al. (2013) and
159 Garcia-Pichel et al. (2013) studies 15% and 23%, respectively, of *Cyanobacteria* sequences are annotated
160 as belonging to "Subsection IV".

4 DISCUSSION

161 BSC N-fixation has long been attributed to heterocystous *Cyanobacteria* and molecular surveys of BSC
162 *nifH* gene content have been consistent with this hypothesis finding cyanobacterial *nifH* types to be
163 numerically dominant in *nifH* gene clone libraries from BSC (Yeager et al., 2006, 2004, 2012). However,
164 $^{15}N_2$ DNA-SIP revealed non-cyanobacterial microorganisms fixed N_2 in early successional BSC samples.
165 DNA from early successional BSC samples–incubated for 2 and 4 days in the presence or absence of
166 $^{15}N_2$–was collected and separated by bouyant density in CsCl density gradients. Heavy CsCl gradient
167 fractions from gradients with ^{15}N-labelled DNA were different in phylogenetic membership/structure
168 than heavy fractions with unlabeled DNA (Figure 1 and Figure S1)). Further, heavy gradient fractions
169 clustered by DNA type (labeled or control) (Figure 1). Therefore, headspace $^{15}N_2$ in early successional
170 BSC microcosms was incorporated into DNA. Further, OTUs enriched in labeled gradient heavy fractions
171 relative to control are the specific taxa that incorporated ^{15}N (from $^{15}N_2$) into biomass. *Proteobacteria*
172 and *Clostridiaceae* represented most OTUs enriched in DNA from labeled gradient heavy fractions
173 relative to control as revealed by a robust statistical framework for quantifying and evaluating differential
174 OTU abundance in microbiome studies (McMurdie and Holmes, 2014; Love et al., 2014). Additionally,
175 *Proteobacteria* and *Clostridiaceae* represented OTUs that most strongly responded to ^{15}N.

176 We propose three mechanisms that could bias *nifH* clone libraries against heteroptophic diazotrophs.
177 First, polyploidy in *Cyanobacteria* (Griese et al., 2011) would inflate the representation of cyanobacteria
178 in community DNA (beyond a cell ratio). Second, *nifH* PCR primers could be biased against heterotrophic
179 diazotrophs. In general the nifH PCR primers used by Yeager et al. (2006, 2004, 2012) ("19F" and
180 "nifH3") for the first round of nested PCR have broad specificity and display at least 86% *in silico*
181 coverage for *Proteobacteria, Cyanobacteria* and "Cluster III" (which includes clostridial *nifH*) reference
182 *nifH* sequences (Gaby and Buckley, 2012). In the second round of the nested PCR protocol used by Yeager
183 et al. (2006, 2004, 2012), primer "nifH11" is' biased against "Cluster III" (50% *in silico* coverage of
184 reference *nifH* sequences) relative to *Proteobacteria* (79% coverage) and *Cyanobacteria* (67% coverage),
185 and, primer "nifH22" matches *Proteobacteria*, *Cyanobacteria* and "Cluster III" reference sequences
186 poorly (16%, 23% and 21% *in silico* coverage, respectively) (Gaby and Buckley, 2012). Unfortunately, it
187 is difficult to assess or quantify this bias (in either direction) without knowing the *nifH* gene content *de*
188 *novo*. Third, heterocysts (the specialized N-fixing cells along the trichome of filamentous heterocystous
189 *Cyanobacteria* such as *Nostoc* and *Scytonema*) may be overrepresented (above a cell ratio) in *nifH* clone
190 libraries. Heterocysts make up a fraction of cells along a trichome and even the non-heterocyst (non-N-
191 fixing) cells in the trichome will possess the *nifH* gene. As a result of polyploidy and the frequency of
192 heterocysts in a cyanobacterial filament, the ratio of cyanobacterial to heterotroph *nifH* gene copies may
193 be 10^2-10^3 higher than the ratio of heterocysts to heterotrophic diazotroph cells. Regardless, our results
194 suggest that BSC N-fixation may include a significant non-cyanobacterial component that requires further
195 assessment across a more comprehensive sampling of BSC types.

196 We did not observe evidence for N-fixation by heterocystous *Cyanobacteria* in the early successional
197 BSC samples used in this study. One possible explanation for our results is that the early successional
198 BSC samples used in this study possessed too few heterocystous *Cyanobacteria* to statistically evaluate
199 their ^{15}N-incorporation. Indeed, only 0.29% of sequences from this study's DNA-SIP 16S rRNA gene
200 sequence collections were from heterocystous *Cyanobacteria* (see results) as opposed to 15% and 23% of
201 total sequences in the Steven et al. (2013) and Garcia-Pichel et al. (2013) data, respectively. Nonetheless,
202 we would still expect even low abundance diazotrophs to show evidence for ^{15}N-incorporation, provided
203 sequence counts were not too sparse in heavy fractions. The OTUs defined by selected heterocystous
204 *Cyanobacteria* sequences presented in Yeager et al. (2006), however, all fall below the sparsity threshold
205 used in our analysis (see methods). Given the sparsity of heterocystous *Cyanobacteria* sequences in
206 the DNA-SIP data set, it is not possible to assess whether heterocystous *Cyanobacteria* incorporated
207 ^{15}N during the incubation. It should be noted that early successional BSC samples possess much less
208 heterocystous *Cyanobacteria* in general (Figure S3) so the samples used in this study are not necessarily

209 unrepresentative of typical early successional BSC simply because they are lacking heterocystous
210 *Cyanobacteria*.

211 The OTUs that did appear to incorporate ^{15}N during the incubation were predominantly *Proteobacteria*
212 and *Firmicutes*. The *Proteobacteria* OTUs for which ^{15}N-incorporation signal was strongest all shared
213 high sequence identity ($>=$98.48%) with 16S sequences from cultivars in genera with known diazotrophs
214 (Table 1). The *Firmicutes* that displayed signal for ^{15}N-incorporation (predominantly *Clostridiaceae*)
215 were not closely related to any cultivars (Table 1, Figure 5). These BSC *Clostrodiaceae* diazotrophs
216 represent a gap in culture collections. Assessing the physiological response of these diazotrophic
217 *Clostridiaceae* to temperature would be useful for predicting how climate change will affect the BSC
218 nitrogen budget.

219 Although too undersampled in the environmental data sets to reach statistical conclusions, ^{15}N-
220 responsive OTUs were found more often in sub-crust or or early successional BSC samples as opposed
221 to crust or mature samples (Figure 2 and Figure S5). This result generates some hypotheses that are
222 counter to prior discussions regarding BSC diazotroph temporal dynamics. Specifically, the succession
223 of BSC may not mark the *emergence* of diazotrophs in BSC but rather the *transition* of the diazotroph
224 community from heterotroph to heterocystous *Cyanobacteria* dominance. Additionally, sub-biocrust soil
225 may contribute significantly to the arid ecosystem N budget.

226 We propose that fast-growing heterotrophic diazotrophs such as *Clostridiaceae* are likely BSC
227 ecosystem pioneers. *M. vaginatus* accumulates compatible solutes such as trehalose and sucrose as
228 osmoprotectants during dessication (Rajeev et al., 2013). Additionally, although not demonstrated
229 specifically with *M. vaginatus*, microorganisms can rapidly excrete compatible solutes upon wetting
230 (Poolman and Glaasker, 1998). Many *Clostridiaceae* have a saccharolytic metabolism (Wiegel et al.,
231 2006) and *Clostridiaceae* isolates have been shown to utilize trehalose and/or sucrose (summarized in
232 Wiegel et al. (2006)). Further, *Clostridiaceae* isolates are fast-growing (doubling times typically between
233 30 min and 3 hr when grown on monosaccharides in culture (Wiegel et al., 2006)). Upon wetting, the early
234 successional BSC environment may become rapidly rich in compatible solutes excreted by *M. vaginatus*.
235 This boom-bust cycle would favor fast-growing microorganisms such as *Clostridiaceae* that can double
236 rapidly and also fix N.

237 Rarefaction curves of all samples from Steven et al. (2013) and Garcia-Pichel et al. (2013) are still
238 sharply increasing especially for sub-crust samples (Figure S4). Parametric richness estimates of BSC
239 diversity indicate the Steven et al. (2013) and Garcia-Pichel et al. (2013) sequencing efforts recovered on
240 average 40.5% (sd. 9.99%) and 45.5% (sd. 11.6%) of predicted 16S OTUs from samples (inset Figure S4),
241 respectively. Therefore, is not alarming that few of the ^{15}N-responsive OTUS were found by Garcia-Pichel
242 et al. (2013) and Steven et al. (2013). Even next-generation sequencing efforts of BSC 16S rRNA genes
243 have only shallowly sampled the full diversity of BSC microbes.

4.1 CONCLUSION

244 Heterocystous *Cyanobacteria* are key contributors to the BSC N-budget, but, the ^{15}N-responsive OTUs
245 found in this study and the *nifH* gene sequences from Steppe et al. (1996) in addition to the N-fixation
246 rate data presented by Johnson et al. (2005) suggest there may be significant non-cyanobacterial BSC
247 diazotrophs specifically within the *Clostrideaceae* and *Proteobacteria*. It seems clear that heterocystous
248 *Cyanobacteria* increase in abundance with BSC age (Yeager et al., 2004). It is less clear if this transition
249 marks the emergence of diazotrophs versus a re-structuring of the BSC diazotroph community from one
250 dominated by *Clostridiaceae* and *Proteobacteria* to one predominantly heterocystous *Cyanobacteria*.
251 DNA-SIP is a valuable tool in the molecular microbial ecologist's toolbox for identifying members of
252 microbial community functional guilds (Neufeld et al., 2007). PCR-based surveys of diagnostic marker
253 genes and DNA-SIP are both used to connect microbial phylogenetic types to microbial activities, but
254 they occupy a non-overlapping set of strengths and weaknesses. DNA-SIP does not focus on a specific
255 diagnostic marker but does identify *active* players in the studied process (i.e. N-fixation). Combined these

256 tools can powerfully reveal connections between ecosystem membership/structure and function. Here we
257 supplement previous surveys of BSC *nifH* diversity, a diagnostic marker PCR-driven approach, with ^{15}N$_2$
258 DNA-SIP, While we do not confirm previous results, we expand knowledge of BSC diazotroph diversity.
259 Predicting BSC N-fixation with respect to climate change, althered precipitation regimes and physical
260 disturbance requires a careful accounting of diazotrophs including non-cyanobacterial types.

5 MATERIALS AND METHODS

5.1 BSC SAMPLING AND INCUBATION CONDITIONS

261 DNA was extracted from 1 g of BSC. Samples were taken from Green Butte, Arizona as previously
262 described (site CP3, Beraldi-Campesi et al. (2009)). All samples were from early successional crusts
263 as described by Johnson et al. (2005). Early successional BSC samples (37.5 cm^2, average mass 35 g)
264 were incubated in sealed chambers under controlled atmosphere and in the light for 4 days. Crusts were
265 sampled and transported while dry and wetted at initiation of the experiment. Treatments included an
266 unlabeled control air headspace and ^{15}N$_2$ enriched air (>98% atom ^{15}N$_2$) headspace. Samples were taken
267 at 2 days and 4 days incubation. Acetylene reduction rates were measured daily. Acetylene reduction
268 rates increased over the course of the experiment (0.8, 4.8, 8.8, and 14.5 μm m^{-2} hr^{-1} ethylene for days
269 1 through 4, respectively).

5.2 DNA EXTRACTION

270 DNA from each sample was extracted using a MoBio PowerSoil DNA Isolation Kit (following
271 manufacturers protocol, but substituting a 2 minute bead beating for the vortexing step), and then gel
272 purified to select high molecular weight DNA (>4 kb) using a 1% low melt agarose gel and β-agarase I
273 for digestion (manufacturer's protocol, NEB, M0392S). Extracts were quantified using PicoGreen nucleic
274 acid quantification dyes (Molecular Probes).

5.3 DNA-SIP

275 CsCl density gradients were formed in 4.7 mL polyallomer centrifuge tubes filled with gradient buffer
276 (15mM Tris-HCl, pH 8; 15mM EDTA; 15mM KCl) which contained 1.725 g/mL CsCl. CsCl density
277 was checked with a digital refractometer as described below. A total of 2.5-5 ug of DNA was added to
278 each tube, and the tubes mixed, prior to centrifugation. Centrifugation was performed in a TLA-110 fixed
279 angle rotor (Beckman Coulter) at 20C for 67 hours at 55,000 rpm. (Buckley et al., 2007). Centrifuged
280 gradients were fractionated from bottom to top in 36 equal fractions of 100 μL, using a by syringe
281 pump as described previously CITE. The density of each fraction was determined using using an AR200
282 refractometer modified to accomidate 5ul samples as described previously (Buckley et al., 2007). DNA
283 in each fraction was desalted on a filter plate (PALL, AcroPrep Advance 96 Filter Plate, Product Number
284 8035), using four washes with 300μL TE per fraction. After each wash, the filter plate was centrifuged at
285 500 g for 10 minutes, with a final spin of 20 minutes. Fractions were resuspended in 50 uL of TE buffer.

5.4 PCR, LIBRARY NORMALIZATION AND DNA SEQUENCING

286 Barcoded PCR of bacterial and archaeal 16S rRNA genes, in preparation for 454 pyrosequencing, was
287 carried out using primer set 515F/806R (Walters et al., 2011) (primers purchased from Integrated DNA
288 Technologies). The primer 806R contained an 8 bp barcode sequence, a "TC" linker, and a Roche 454
289 B sequencing adaptor, while the primer 515F contained the Roche 454 A sequencing adapter. Each
290 25 μL reaction contained 1x PCR Gold Buffer (Roche), 2.5 mM MgCl$_2$, 200 μM of each of the four
291 dNTPs (Promega), 0.5 mg/mL BSA (New England Biolabs), 0.3 μM of each primers, 1.25 U of Amplitaq

292   Gold (Roche), and 8 μL of template. Each sample was amplified in triplicate. Thermal cycling occurred
293   with an initial denaturation step of 5 minutes at 95C, followed by 40 cycles of amplification (20s at
294   95C, 20s at 53C, 30s at 72C), and a final extension step of 5 min at 72C. Triplicate amplicons were
295   pooled and purified using Agencourt AMPure PCR purification beads, following manufacturers protocol.
296   Once purified, amplicons were quantified using PicoGreen nucleic acid quantification dyes (Molecular
297   Probes) and pooled together in equimolar amounts. Samples were sent to the Environmental Genomics
298   Core Facility at the University of South Carolina (now Selah Genomics) to be run on a Roche FLX 454
299   pyrosequencing machine (FLX-Titanium platform).

5.5   DATA ANALYSIS

300   *5.5.1   Sequence quality control*   Sequences were initially screened by maximum expected errors at a
301   specific read length threshold (Edgar, 2013) which has been shown to be as effective as denoising with
302   respect to removing pyrosequencing errors. Specifically, reads were first truncated to 230 nucleotides
303   (nt) (all reads shorter than 230 nt were discarded) and any read that exceeded a maximum expected
304   error threshold of 1.0 was removed. After truncation and max expected error trimming, 91% of original
305   reads remained. Forward primer and barcode was then removed from the high quality, truncated reads.
306   Remaining reads were taxonomically annotated using the "UClust" taxonomic annotation framework in
307   the QIIME software package (Caporaso et al., 2010; Edgar, 2010) with cluster seeds from Silva SSU
308   rRNA database (Pruesse et al., 2007) 97% sequence identity OTUs as reference (release 111Ref). Reads
309   annotated as "Chloroplast", "Eukaryota", "Archaea", "Unassigned" or "mitochondria" were culled from
310   the dataset. Finally, reads were aligned to the Silva reference alignment provided by the Mothur software
311   package (Schloss et al., 2009) using the Mothur NAST aligner (DeSantis et al., 2006). All reads that
312   did not align to the expected amplicon region of the SSU rRNA gene were discarded. Quality control
313   parameters removed 34,716 of 258,763 raw reads.

314   *5.5.2   Sequence clustering*   Sequences were distributed into OTUs using the UParse methodology
315   (Edgar, 2013). Specifically, cluster seeds were identified using USearch on non-redundant reads sorted by
316   count. The sequence identity threshold for establishing a new OTU centroid was 97%. After initial cluster
317   centroid selection, select 16S rRNA gene sequences from Yeager et al. (2006) were added to the centroid
318   collection. Specifically, Yeager et al. (2006) Colorado Plateau or Moab, Utah sequences were added
319   which included the 16S rRNA gene sequences for *Calothrix* MCC-3A (accession DQ531700.1), *Nostoc*
320   *commune* MCT-1 (accession DQ531903), *Nostoc commune* MFG-1 (accession DQ531699.1), *Scytonema*
321   *hyalinum* DC-A (accession DQ531701.1), *Scytonema hyalinum* FGP-7A (accession DQ531697.1),
322   *Spirirestis rafaelensis* LQ-10 (accession DQ531696.1). Centroid sequences that matched selected Yeager
323   et al. (2006) sequences with greater than to 97% sequence identity were subsequently removed from the
324   centroid collection. With USearch/UParse, potential chimeras are identified during OTU centroid selection
325   and are not allowed to become cluster centroids effectively removing chimeras from the read pool. All
326   quality controlled reads were then mapped to cluster centroids at an identity threshold of 97% again using
327   USearch. A total of 95.6% of quality controlled reads could be mapped to centroids. Unmapped reads
328   do not count towards sample counts and are removed from downstream analyses. The USearch software
329   version for cluster generation was 7.0.1090. Garcia-Pichel et al. (2013) and Steven et al. (2013)) sequences
330   were quality screened by alignment coordinates(described above) and included as input to USearch for
331   OTU centroid selection and subsequent mapping to OTU centroids.

332   *5.5.3   Phylogenetic tree*   The alignment for the *Clostridiaceae* phylogeny was created using SSU-Align
333   which is based on Infernal (Nawrocki and Eddy, 2013; Nawrocki et al., 2009). Columns in the alignment
334   that were not included in the SSU-Align covariance models or were aligned with poor confidence (less
335   than 95% of characters in a position had posterior probability alignment scores of at least 95%) were
336   masked for phylogenetic reconstruction. Additionally, the alignment was trimmed to coordinates such
337   that all sequences in the alignment began and ended at the same positions. The *Clostridiaceae* tree

338 included all top BLAST hits (parameters below) for [15]N *Clostridiaceae* responders in the Living Tree
339 Project database (Yarza et al., 2008) in addition to BLAST hits within a sequence identity threshold of
340 97% to ^{15}N responders from the Silva SSURef_NR SSU rRNA database (Pruesse et al., 2007). Only one
341 SSURef_NR115 hit per study per OTU (the study was determined by "title" field) was selected for the
342 tree. FastTree (Price et al., 2010) was used to build the tree and support values are SH-like scores reported
343 by FastTree. Short sequences were mapped to the reference backbone using pplacer (Matsen et al., 2010)
344 (default parameters). pplacer finds the edge placements that maximize phylogenetic likelihood. Prior to
345 being mapped to the reference tree, short sequences were aligned to the reference alignment using Infernal
346 (Nawrocki et al., 2009) against the same SSU-Align covariance model used to align reference sequences.

347 *5.5.4 Identifying OTUs that incorporated ^{15}N into their DNA*   DNA-SIP is a culture-independent
348 approach towards defining identity-function connections in microbial communities (Buckley, 2011;
349 Neufeld et al., 2007; Radajewski and Murrell, 2001). Microbes participating in a specific process
350 are identified on the basis of isotope assimilation into DNA. Isotopically labeled nucleic acids can
351 be separated from unlabeled by buoyant density in a CsCl gradient. As the buoyant density of a
352 macromolecule is dependent on many factors in addition to stable isotope incorporation (e.g. GC-content
353 in nucleic acids (Youngblut and Buckley, 2014)), labeled nucleic acids from one microbial population
354 may have the same buoyant density of unlabeled nucleic acids from another. Therefore it is imperative
355 to compare density gradients with nucleic acids from heavy stable isotope incubations to gradients
356 from "control" incubations where everything mimics the experimental conditions except that unlabeled
357 substrates are used. By contrasting heavy density gradient fractions in experimental density gradients
358 (hereafter referred to as "labeled" gradients) against heavy fractions in control gradients, the identities of
359 microbes with labeled nucleic acids can be determined

360   We used an RNA-Seq differential expression statistical framework (Love et al., 2014) to find OTUs
361 enriched in heavy fractions of labeled gradients relative to corresponding density fractions in control
362 gradients (for review of RNA-Seq differential expression statistics applied to microbiome OTU count data
363 see McMurdie and Holmes (2014)). We use the term differential abundance (coined by McMurdie and
364 Holmes (2014)) to denote OTUs that have different proportion means across sample classes (in this case
365 the only sample class is labeled/control). CsCl gradient fractions were categorized as "heavy" or "light".
366 The heavy category denotes fractions with density values above 1.725 g/mL. Since we are only interested
367 in enriched OTUs (labeled versus control), we used a one-sided z-test for differential abundance (the null
368 hypothesis is the labeled:control proportion mean ratio for an OTU is less than a selected threshold). P-
369 values were corrected with the Benjamini and Hochberg method (Benjamini and Hochberg, 1995). We
370 selected a $\log_2$ fold change null threshold of 0.25 (or a labeled:control proportion mean ratio of 1.19).
371 DESeq2 was used to calculate the moderated $\log_2$ fold change of labeled:control proportion mean ratios
372 and corresponding standard errors. Mean ratio moderation allows for reliable ratio ranking such that high
373 variance and likely statistically insignificant mean ratios are appropriately shrunk and subsequently ranked
374 lower than they would be as raw ratios. Those OTUs that exhibit a statistically significant increase in
375 proportion in heavy fractions from $^{15}N_2$-labeled samples relative to corresponding controls have increased
376 significantly in bouyant density in response to $^{15}N_2$ treatment; a response that is expected for N_2-fixing
377 organisms.

378 *5.5.5 Community and Sequence Analysis*   BLAST searches were done with the "blastn" program from
379 BLAST+ toolkit (Camacho et al., 2009) version 2.2.29+. Default parameters were always employed and
380 the BioPython (Cock et al., 2009) BLAST+ wrapper was used to invoke the blastn program. Pandas
381 (McKinney, 2012) and dplyr (Wickham and Francois, 2014) were used to parse and munge BLAST output
382 tables.

383   Principal coordinate ordinations depict the relationship between samples at each time point (day 2
384 and 4). Bray-Curtis distances were used as the sample distance metric for ordination. The Phyloseq
385 (McMurdie and Holmes, 2014) wrapper for Vegan (Oksanen et al., 2013) (both R packages) was used

386 to compute sample values along principal coordinate axes. GGplot2 (Wickham, 2009) was used to display
387 sample points along the first and second principal axes. Adonis tests Anderson (2001) were done with
388 default number of permutations (1000).

389 Rarefaction curves were created using bioinformatics modules in the PyCogent Python package (Knight
390 et al., 2007). Parametric richness estimates were made with CatchAll using only the best model for total
391 OTU estimates (Bunge, 2010).

392 All code to take raw sequencing data through the presented figures can be found at:

393 `http://nbviewer.ipython.org/github/chuckpr/NSIP_data_analysis`

REFERENCES

394 Marti J. Anderson. A new method for non-parametric multivariate analysis of variance. *Austral Ecology*,
395   26(1):32–46, 2001. doi: 10.1111/j.1442-9993.2001.01070.pp.x. URL `http://dx.doi.org/10.`
396   `1111/j.1442-9993.2001.01070.pp.x`.
397 J. Belnap. Factors Influencing Nitrogen Fixation and Nitrogen Release in Biological Soil Crusts.
398   In *Biological Soil Crusts: Structure Function, and Management*, pages 241–261. Springer
399   Science, 2001. doi: 10.1007/978-3-642-56475-8_19. URL `http://dx.doi.org/10.1007/`
400   `978-3-642-56475-8_19`.
401 J. Belnap. Factors Influencing Nitrogen Fixation and Nitrogen Release in Biological Soil Crusts. In
402   Jayne Belnap and OttoL. Lange, editors, *Biological Soil Crusts: Structure, Function, and Management*,
403   volume 150 of *Ecological Studies*, pages 241–261. Springer Berlin Heidelberg, 2003. ISBN 978-
404   3-540-43757-4. doi: 10.1007/978-3-642-56475-8_19. URL `http://dx.doi.org/10.1007/`
405   `978-3-642-56475-8_19`.
406 J. Belnap, R. Prasse, and K.T. Harper. Influence of Biological Soil Crusts on Soil Environments and
407   Vascular Plants. In Jayne Belnap and OttoL. Lange, editors, *Biological Soil Crusts: Structure, Function,*
408   *and Management*, volume 150 of *Ecological Studies*, pages 281–300. Springer Berlin Heidelberg, 2003.
409   ISBN 978-3-540-43757-4. doi: 10.1007/978-3-642-56475-8_21. URL `http://dx.doi.org/10.`
410   `1007/978-3-642-56475-8_21`.
411 Jayne Belnap. Nitrogen fixation in biological soil crusts from southeast Utah USA. *Biology and Fertility*
412   *of Soils*, 35(2):128–135, 2002. doi: 10.1007/s00374-002-0452-x. URL `http://dx.doi.org/10.`
413   `1007/s00374-002-0452-x`.
414 Jayne Belnap. Some Like It Hot, Some Not. *Science*, 340(6140):1533–1534, 2013. doi: 10.1126/science.
415   1240318. URL `http://www.sciencemag.org/content/340/6140/1533.short`.
416 Yoav Benjamini and Yosef Hochberg. Controlling the False Discovery Rate: A Practical and Powerful
417   Approach to Multiple Testing. *Journal of the Royal Statistical Society. Series B (Methodological)*, 57
418   (1):289–300, 1995. ISSN 00359246. doi: 10.2307/2346101. URL `http://dx.doi.org/10.`
419   `2307/2346101`.
420 H. Beraldi-Campesi, H. E. Hartnett, A. Anbar, G. W. Gordon, and F. Garcia-Pichel. Effect of biological
421   soil crusts on soil elemental concentrations: implications for biogeochemistry and as traceable
422   biosignatures of ancient life on land. *Geobiology*, 7(3):348–359, 2009. doi: 10.1111/j.1472-4669.
423   2009.00204.x. URL `http://dx.doi.org/10.1111/j.1472-4669.2009.00204.x`.
424 J. Roger Bray and J. T. Curtis. An Ordination of the Upland Forest Communities of Southern Wisconsin.
425   *Ecological Monographs*, 27(4):325, 1957. doi: 10.2307/1942268. URL `http://dx.doi.org/`
426   `10.2307/1942268`.
427 Daniel H. Buckley. Stable Isotope Probing Techniques Using 15N. In *Stable Isotope Probing and Related*
428   *Technologies*, pages 129–147. American Society of Microbiology, 2011. doi: 10.1128/9781555816896.
429   ch7. URL `http://dx.doi.org/10.1128/9781555816896.ch7`.
430 DH Buckley, V Huangyutitham, SF Hsu, and TA Nelson. Stable isotope probing with 15N2 reveals novel
431   noncultivated diazotrophs in soil. *Appl Environ Microbiol*, 73:3196–204, 2007.

432 John Bunge. Estimating the Number of Species with Catchall. In *Biocomputing 2011*, pages 121–130.
433   World Scientific, 2010. doi: 10.1142/9789814335058_0014. URL `http://dx.doi.org/10.`
434   `1142/9789814335058_0014`.
435 C Camacho, G Coulouris, V Avagyan, N Ma, J Papadopoulos, K Bealer, and TL Madden. BLAST+:
436   architecture and applications. 10:421, 2009.
437 JG Caporaso, J Kuczynski, J Stombaugh, K Bittinger, FD Bushman, EK Costello, N Fierer, AG Pea,
438   JK Goodrich, JI Gordon, GA Huttley, ST Kelley, D Knights, JE Koenig, RE Ley, CA Lozupone,
439   D McDonald, BD Muegge, M Pirrung, J Reeder, JR Sevinsky, PJ Turnbaugh, WA Walters, J Widmann,
440   T Yatsunenko, J Zaneveld, and R Knight. QIIME allows analysis of high-throughput community
441   sequencing data. 7:335–6, 2010.
442 PJ Cock, T Antao, JT Chang, BA Chapman, CJ Cox, A Dalke, I Friedberg, T Hamelryck, F Kauff,
443   B Wilczynski, and Hoon MJ de. Biopython: freely available Python tools for computational molecular
444   biology and bioinformatics. 25:1422–3, 2009.
445 TZ Jr DeSantis, P Hugenholtz, K Keller, EL Brodie, N Larsen, YM Piceno, R Phan, and GL Andersen.
446   NAST: a multiple sequence alignment server for comparative analysis of 16S rRNA genes. 34:W394–9,
447   2006.
448 RC Edgar. Search and clustering orders of magnitude faster than BLAST. 26:2460–1, 2010.
449 RC Edgar. UPARSE: highly accurate OTU sequences from microbial amplicon reads. 10:996–8, 2013.
450 R. D. Evans and J. Belnap. Long-Term Consequences of Disturbance on Nitrogen Dynamics in an
451   Arid Ecosystem. *Ecology*, 80(1):150–160, 1999. doi: 10.1890/0012-9658(1999)080[0150:ltcodo]2.
452   0.co;2. URL `http://dx.doi.org/10.1890/0012-9658(1999)080[0150:LTCODO]2.`
453   `0.CO;2`.
454 R. D. Evans and O. L. Lange. Biological Soil Crusts and Ecosystem Nitrogen and Carbon
455   Dynamics. In *Biological Soil Crusts: Structure Function, and Management*, pages 263–279. Springer
456   Science, 2001. doi: 10.1007/978-3-642-56475-8_20. URL `http://dx.doi.org/10.1007/`
457   `978-3-642-56475-8_20`.
458 John Christian Gaby and Daniel H. Buckley. A Comprehensive Evaluation of PCR Primers to Amplify
459   the nifH Gene of Nitrogenase. *PLoS ONE*, 7(7):e42149, 2012. doi: 10.1371/journal.pone.0042149.
460   URL `http://dx.doi.org/10.1371/journal.pone.0042149`.
461 F. Garcia-Pichel, S. L. Johnson, D. Youngkin, and J. Belnap. Small-Scale Vertical Distribution of Bacterial
462   Biomass and Diversity in Biological Soil Crusts from Arid Lands in the Colorado Plateau. *Microbial*
463   *Ecology*, 46(3):312–321, 2003a. doi: 10.1007/s00248-003-1004-0. URL `http://dx.doi.org/`
464   `10.1007/s00248-003-1004-0`.
465 F. Garcia-Pichel, V. Loza, Y. Marusenko, P. Mateo, and R. M. Potrafka. Temperature Drives the
466   Continental-Scale Distribution of Key Microbes in Topsoil Communities. *Science*, 340(6140):1574–
467   1577, 2013. doi: 10.1126/science.1236404. URL `http://dx.doi.org/10.1126/science.`
468   `1236404`.
469 Ferran Garcia-Pichel, Jayne Belnap, Susanne Neuer, and Ferdinand Schanz. Estimates of global
470   cyanobacterial biomass and its distribution. *Algological Studies*, 109(1):213–227, 2003b.
471 Marco Griese, Christian Lange, and Jrg Soppa. Ploidy in cyanobacteria. *FEMS Microbiology Letters*,
472   323(2):124–131, 2011. doi: 10.1111/j.1574-6968.2011.02368.x. URL `http://dx.doi.org/10.`
473   `1111/j.1574-6968.2011.02368.x`.
474 SL Johnson, CR Budinoff, J Belnap, and F Garcia-Pichel. Relevance of ammonium oxidation within
475   biological soil crust communities. 7:1–12, 2005.
476 A. Karnieli, R.F. Kokaly, N.E. West, and R.N. Clark. Remote Sensing of Biological Soil Crusts. In
477   Jayne Belnap and OttoL. Lange, editors, *Biological Soil Crusts: Structure, Function, and Management*,
478   volume 150 of *Ecological Studies*, pages 431–455. Springer Berlin Heidelberg, 2003. ISBN 978-
479   3-540-43757-4. doi: 10.1007/978-3-642-56475-8_31. URL `http://dx.doi.org/10.1007/`
480   `978-3-642-56475-8_31`.
481 Rob Knight, Peter Maxwell, Amanda Birmingham, Jason Carnes, J Gregory Caporaso, Brett C Easton,
482   Michael Eaton, Micah Hamady, Helen Lindsay, Zongzhi Liu, Catherine Lozupone, Daniel McDonald,
483   Michael Robeson, Raymond Sammut, Sandra Smit, Matthew J Wakefield, Jeremy Widmann, Shandy
484   Wikman, Stephanie Wilson, Hua Ying, and Gavin A Huttley. {PyCogent}: a toolkit for making sense

485 from sequence. *Genome Biol*, 8(8):R171, 2007. doi: 10.1186/gb-2007-8-8-r171. URL http://dx.
486   doi.org/10.1186/gb-2007-8-8-r171.
487 M. I. Love, W. Huber, and S. Anders. Moderated estimation of fold change and dispersion for {RNA}-Seq
488   data with DESeq2. Technical report, 2014. URL http://dx.doi.org/10.1101/002832.
489 Frederick A Matsen, Robin B Kodner, and E Virginia Armbrust. pplacer: linear time maximum-likelihood
490   and Bayesian phylogenetic placement of sequences onto a fixed reference tree. *BMC Bioinformatics*,
491   11(1):538, 2010. doi: 10.1186/1471-2105-11-538. URL http://dx.doi.org/10.1186/
492   1471-2105-11-538.
493 Wes McKinney. pandas: Python Data Analysis Library. Online, 2012. URL http://pandas.
494   pydata.org/.
495 PJ McMurdie and S Holmes. Waste not, want not: why rarefying microbiome data is inadmissible. 10:
496   e1003531, 2014.
497 EP Nawrocki and SR Eddy. Infernal 1.1: 100-fold faster RNA homology searches. 29:2933–5, 2013.
498 EP Nawrocki, DL Kolbe, and SR Eddy. Infernal 1.0: inference of RNA alignments. 25:1335–7, 2009.
499 JD Neufeld, J Vohra, MG Dumont, T Lueders, M Manefield, MW Friedrich, and JC Murrell. DNA
500   stable-isotope probing. 2:860–6, 2007.
501 Jari Oksanen, F. Guillaume Blanchet, Roeland Kindt, Pierre Legendre, Peter R. Minchin, R. B. O'Hara,
502   Gavin L. Simpson, Peter Solymos, M. Henry H. Stevens, and Helene Wagner. *vegan: Community
503   Ecology Package*, 2013. URL http://CRAN.R-project.org/package=vegan. R package
504   version 2.0-10.
505 Bert Poolman and Erwin Glaasker. Regulation of compatible solute accumulation in bacteria. *Molecular
506   Microbiology*, 29(2):397–407, 1998. doi: 10.1046/j.1365-2958.1998.00875.x. URL http://dx.
507   doi.org/10.1046/j.1365-2958.1998.00875.x.
508 MN Price, PS Dehal, and AP Arkin. FastTree 2–approximately maximum-likelihood trees for large
509   alignments. 5:e9490, 2010.
510 E Pruesse, C Quast, K Knittel, BM Fuchs, W Ludwig, J Peplies, and FO Glckner. SILVA: a comprehensive
511   online resource for quality checked and aligned ribosomal RNA sequence data compatible with ARB.
512   35:7188–96, 2007.
513 Stefan Radajewski and J Colin Murrell. Stable Isotope Probing for Detection of Methanotrophs After
514   Enrichment with 13CH4. In *Gene Probes*, pages 149–157. Humana Press, sep 2001. doi: 10.1385/
515   1-59259-238-4:149. URL http://dx.doi.org/10.1385/1-59259-238-4:149.
516 Lara Rajeev, Ulisses Nunes da Rocha, Niels Klitgord, Eric G Luning, Julian Fortney, Seth D Axen,
517   Patrick M Shih, Nicholas J Bouskill, Benjamin P Bowen, Cheryl A Kerfeld, Ferran Garcia-Pichel,
518   Eoin L Brodie, Trent R Northen, and Aindrila Mukhopadhyay. Dynamic cyanobacterial response to
519   hydration and dehydration in a desert biological soil crust. *The ISME Journal*, 7(11):2178–2191, 2013.
520   doi: 10.1038/ismej.2013.83. URL http://dx.doi.org/10.1038/ismej.2013.83.
521 PD Schloss, SL Westcott, T Ryabin, JR Hall, M Hartmann, EB Hollister, RA Lesniewski, BB Oakley,
522   DH Parks, CJ Robinson, JW Sahl, B Stres, GG Thallinger, Horn DJ Van, and CF Weber.
523   Introducing mothur: open-source, platform-independent, community-supported software for describing
524   and comparing microbial communities. 75:7537–41, 2009.
525 T.F. Steppe, J.B. Olson, H.W. Paerl, R.W. Litaker, and J. Belnap. Consortial N2 fixation: a strategy
526   for meeting nitrogen requirements of marine and terrestrial cyanobacterial mats. *FEMS Microbiology
527   Ecology*, 21(3):149–156, 1996. doi: 10.1111/j.1574-6941.1996.tb00342.x. URL http://dx.doi.
528   org/10.1111/j.1574-6941.1996.tb00342.x.
529 Blaire Steven, La Verne Gallegos-Graves, Jayne Belnap, and Cheryl R. Kuske. Dryland soil microbial
530   communities display spatial biogeographic patterns associated with soil depth and soil parent material.
531   *FEMS Microbiol Ecol*, 86(1):101–113, 2013. doi: 10.1111/1574-6941.12143. URL http://dx.
532   doi.org/10.1111/1574-6941.12143.
533 WA Walters, JG Caporaso, CL Lauber, D Berg-Lyons, N Fierer, and R Knight. PrimerProspector: de novo
534   design and taxonomic analysis of barcoded polymerase chain reaction primers. 27:1159–61, 2011.
535 Hadley Wickham. *ggplot2: elegant graphics for data analysis*. Springer New York, 2009. ISBN 978-0-
536   387-98140-6. URL http://had.co.nz/ggplot2/book.

Hadley Wickham and Romain Francois. *dplyr: dplyr: a grammar of data manipulation*, 2014. URL http://CRAN.R-project.org/package=dplyr. R package version 0.2.

Juergen Wiegel, Ralph Tanner, and Fred A. Rainey. An Introduction to the Family Clostridiaceae. In *The Prokaryotes*, pages 654–678. Springer US, 2006. doi: 10.1007/0-387-30744-3_20. URL http://dx.doi.org/10.1007/0-387-30744-3_20.

Pablo Yarza, Michael Richter, Jörg Peplies, Jean Euzeby, Rudolf Amann, Karl-Heinz Schleifer, Wolfgang Ludwig, Frank Oliver Glöckner, and Ramon Rosselló-Móra. The All-Species Living Tree project: A 16S rRNA-based phylogenetic tree of all sequenced type strains. *Systematic and Applied Microbiology*, 31(4):241–250, 2008. doi: 10.1016/j.syapm.2008.07.001. URL http://dx.doi.org/10.1016/j.syapm.2008.07.001.

Chris M. Yeager, Jennifer L. Kornosky, Rachael E. Morgan, Elizabeth C. Cain, Ferran Garcia-Pichel, David C. Housman, Jayne Belnap, and Cheryl R. Kuske. Three distinct clades of cultured heterocystous cyanobacteria constitute the dominant N2-fixing members of biological soil crusts of the Colorado Plateau USA. *FEMS Microbiology Ecology*, 60(1):85–97, 2006. doi: 10.1111/j.1574-6941.2006.00265.x. URL http://dx.doi.org/10.1111/j.1574-6941.2006.00265.x.

Chris M. Yeager, Cheryl R. Kuske, Travis D. Carney, Shannon L. Johnson, Lawrence O. Ticknor, and Jayne Belnap. Response of Biological Soil Crust Diazotrophs to Season Altered Summer Precipitation, and Year-Round Increased Temperature in an Arid Grassland of the Colorado Plateau, USA. *Front. Microbio.*, 3, 2012. doi: 10.3389/fmicb.2012.00358. URL http://dx.doi.org/10.3389/fmicb.2012.00358.

CM Yeager, JL Kornosky, DC Housman, EE Grote, J Belnap, and CR Kuske. Diazotrophic community structure and function in two successional stages of biological soil crusts from the Colorado Plateau and Chihuahuan Desert. 70:973–83, 2004.

ND Youngblut and DH Buckley. Intra-genomic variation in G+C content and its implications for DNA stable isotope probing (DNA-SIP). 2014.

6 FIGURES AND LONG TABLES

562 **Table 1.**[15]N responders BLAST search against Living Tree Project. Genera of all top BLAST hits are
563 shown.

OTU ID	*Genera*	**BLAST %ID**	*Phylum*
OTU.78	*Desulfocella, Bryobacter*	80.31	*Acidobacteria*
OTU.55	*Desulfocella, Bryobacter*	81.03	*Acidobacteria*
OTU.116	*Streptomyces*	100.0	*Actinobacteria*
OTU.140	*Bacillus*	100.0	*Firmicutes*
OTU.3	*Bacillus*	100.0	*Firmicutes*
OTU.1747	*Clostridium*	94.36	*Firmicutes*
OTU.327	*Clostridium*	94.92	*Firmicutes*
OTU.17	*Clostridium*	95.45	*Firmicutes*
OTU.61	*Clostridium*	95.92	*Firmicutes*
OTU.11	*Clostridium*	95.94	*Firmicutes*
OTU.2175	*Clostridium*	95.96	*Firmicutes*
OTU.1673	*Clostridium*	95.9	*Firmicutes*
OTU.330	*Clostridium*	96.94	*Firmicutes*
OTU.75	*Clostridium*	96.97	*Firmicutes*
OTU.643	*Clostridium*	97.45	*Firmicutes*
OTU.3712	*Clostridium, Eubacterium*	96.43	*Firmicutes*
OTU.37	*Clostridium, Ilyobacter*	96.43	*Firmicutes*
OTU.2404	*Domibacillus*	99.49	*Firmicutes*
OTU.4167	*Fonticella*	93.43	*Firmicutes*
OTU.4037	*Fonticella*	93.85	*Firmicutes*
OTU.57	*Fonticella, Caloramator*	93.88	*Firmicutes*
OTU.575	*Gracilibacter*	94.42	*Firmicutes*
OTU.259	*Parasporobacterium*	98.47	*Firmicutes*
OTU.278	*Symbiobacterium*	90.62	*Firmicutes*
OTU.88	*Symbiobacterium*	92.86	*Firmicutes*
OTU.342	*Acinetobacter*	100.0	*Proteobacteria*
OTU.263	*Azospirillum*	98.48	*Proteobacteria*
OTU.137	*Azospirillum*	98.98	*Proteobacteria*
OTU.176	*Delftia*	100.0	*Proteobacteria*
OTU.14	*Klebsiella, Pantoea, Erwinia, Enterobacter, Kluyvera, Buttiauxella*	99.49	*Proteobacteria*
OTU.586	*Ottowia, Diaphorobacter, Ideonella, Vitreoscilla, Comamonas*	98.48	*Proteobacteria*

Table 1 – continued from previous page

OTU ID	*Genera*	BLAST %ID	*Phylum*
OTU.321	*Pseudomonas*	100.0	*Proteobacteria*
OTU.54	*Shigella, Escherichia*	100.0	*Proteobacteria*

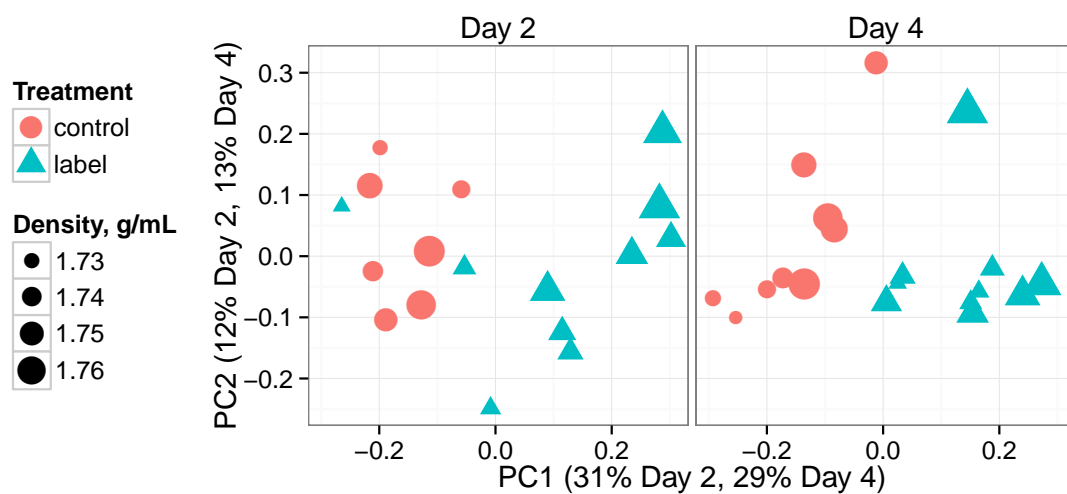**Figure 1.** Ordination of heavy gradient fractions by Bray-Curtis distances on the basis of OTU content.

Figure 2. Phylogenetic trees of OTUs passing sparsity threshold for **A** *Proteobacteria*, **B** *Acidobacteria* and **C** *Firmicutes*. ^{15}N-responders are identified by dots present in column **i**. Log$_2$ of proportion mean ratios (labeled:control samples) for each OTU are presented as a heatmap in column **ii** with results from days 2 and 4 on the left and right sides of the column respectively. High values indicate ^{15}N incorporation. Presence/absence of OTUs (black indicates presence) in lichen, light, or dark environmental samples (Garcia-Pichel et al., 2013) is shown in column **iii**. Presence/absence of OTUs (black indicates presence) in crust and below crust samples (Steven et al., 2013) is shown in column **iv**
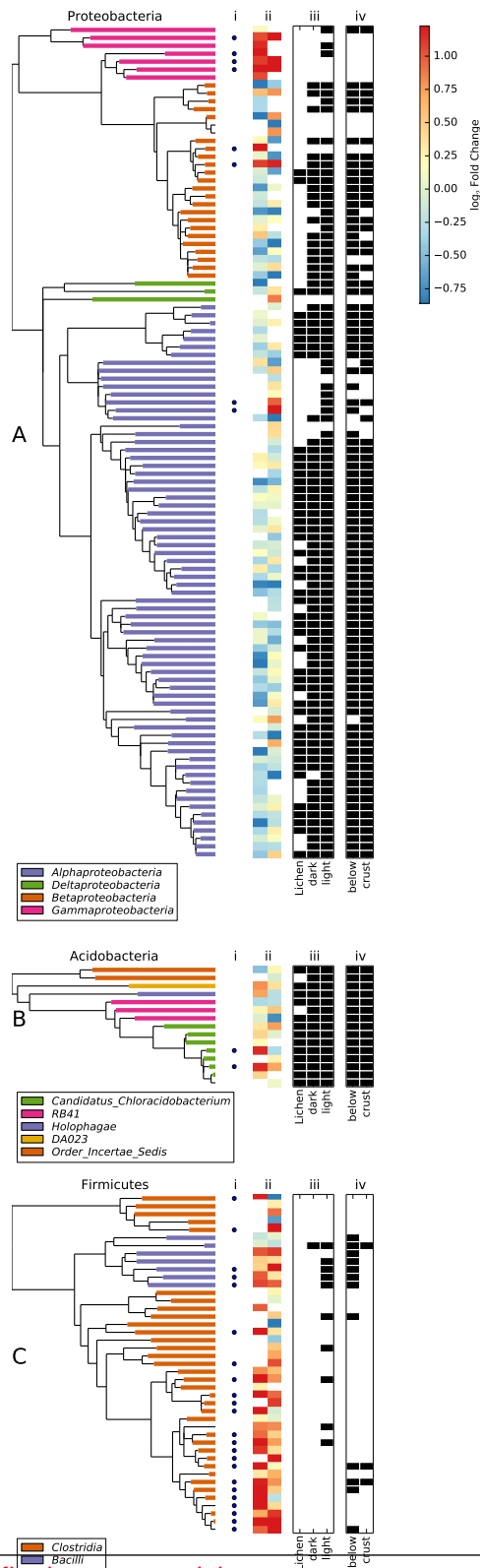
Figure 3. Moderated log$_2$ of proportion mean ratios for labeled versus control gradients (heavy fractions only, densities >1.725 g/mL). All OTUs passing the sparsity treshold (see methods) at a specific incubation day are shown. Red color denotes a proportion mean ratio that has a corresponding adjusted p-value below a false discovery rate of 10% (the null model is that the proportion mean is ratio is below 0.25). The horizontal line is the proportion mean threshold for the null model, 0.25. The inset figure summarizes the taxonomy of OTUs that with proportion mean ratio p-vaules under 0.10 for at least one time point.

Figure 4. Relative abundance values in heavy fractions (density greater or equal to 1.725 g/mL) for the top 10 ^{15}N "responders" (putative diazotrophs, see results for selection criteria of top 10) at each incubation day. See Table 1 for BLAST results against the LTP database (release 115). Point area is proportional to CsCl gradient fraction density, and color signifies control (red) or labeled (blue) treatment.
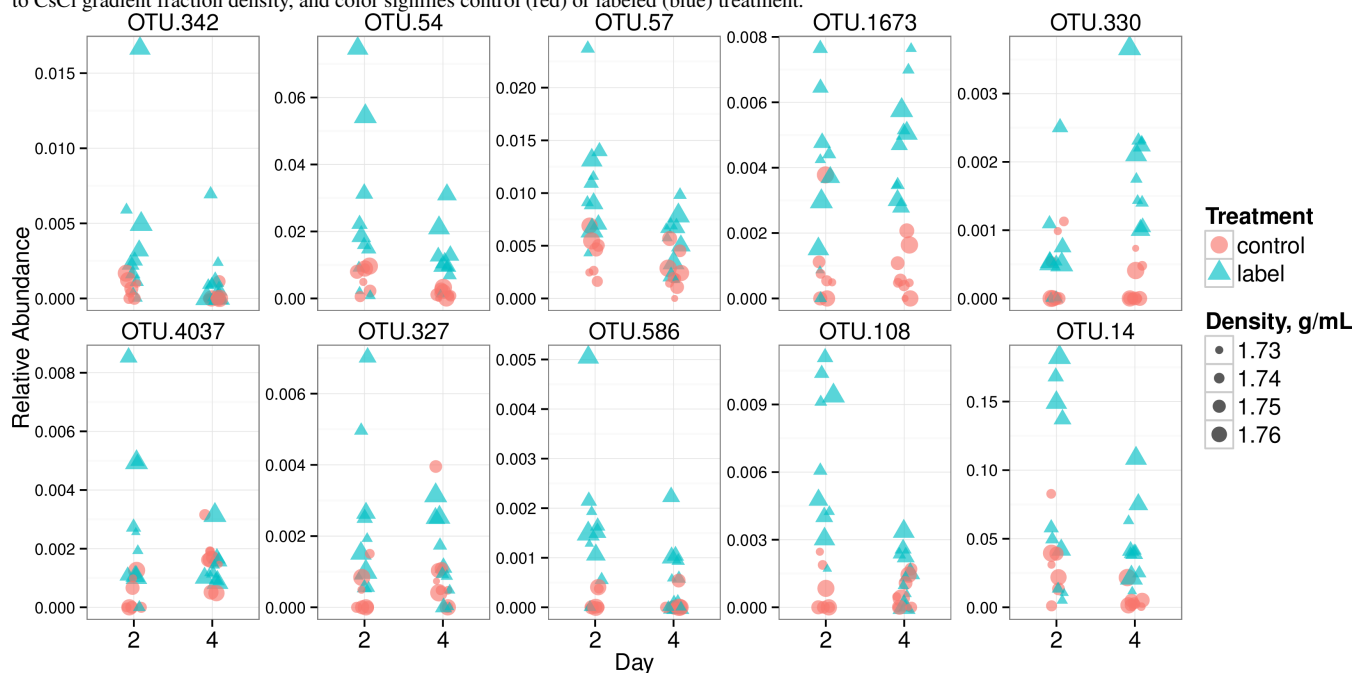
Figure 5. See methods for selection criteria for sequences in backbone tree. Edge width is proportional to number of short putative *Clostridiaceae* diazotroph sequences placed at that position. Placement of short sequences can be spread across multiple edges Matsen et al. (2010). Reference sequences from cultivars have boxes at tips and full species names. Tips with only accession annotations are from environmental reference sequences.
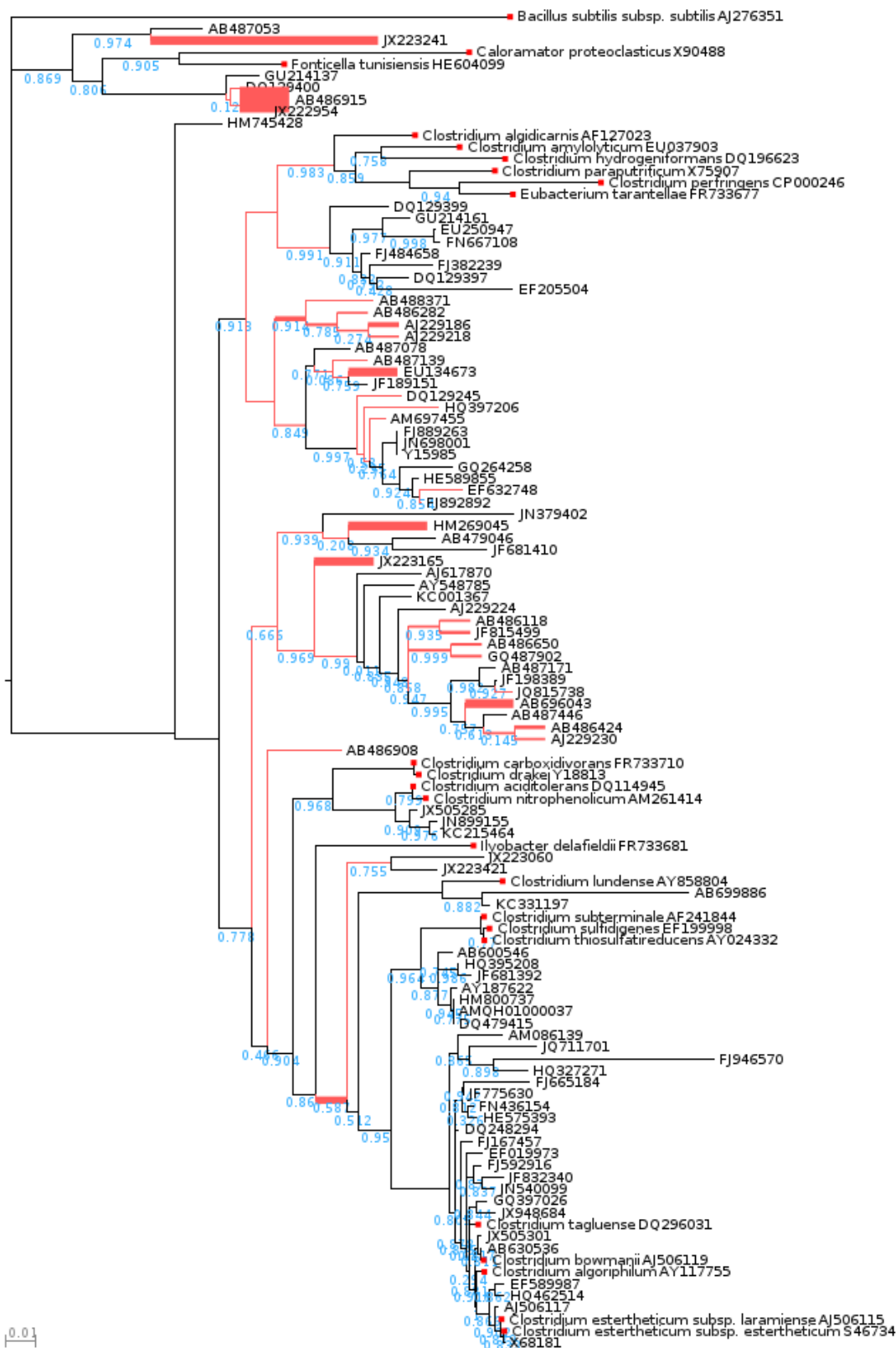
7 SUPPLEMENTAL FIGURES

Figure S1. Ordination of Bray-Curtis sample pairwise distances for each incubation time. Point area is proportional to the density of the CsCl gradient fraction for each sequence library, and color/shape reflects control (red triangles) or labeled (blue circles) treatment. Inset shows Bray-Curtis distances for paired control versus labeled CsCl gradient fractions (i.e. fractions from the same incubation day and same density) against the density of the pair (p-value: $4.526e^{-5}$, r^2: 0.434).
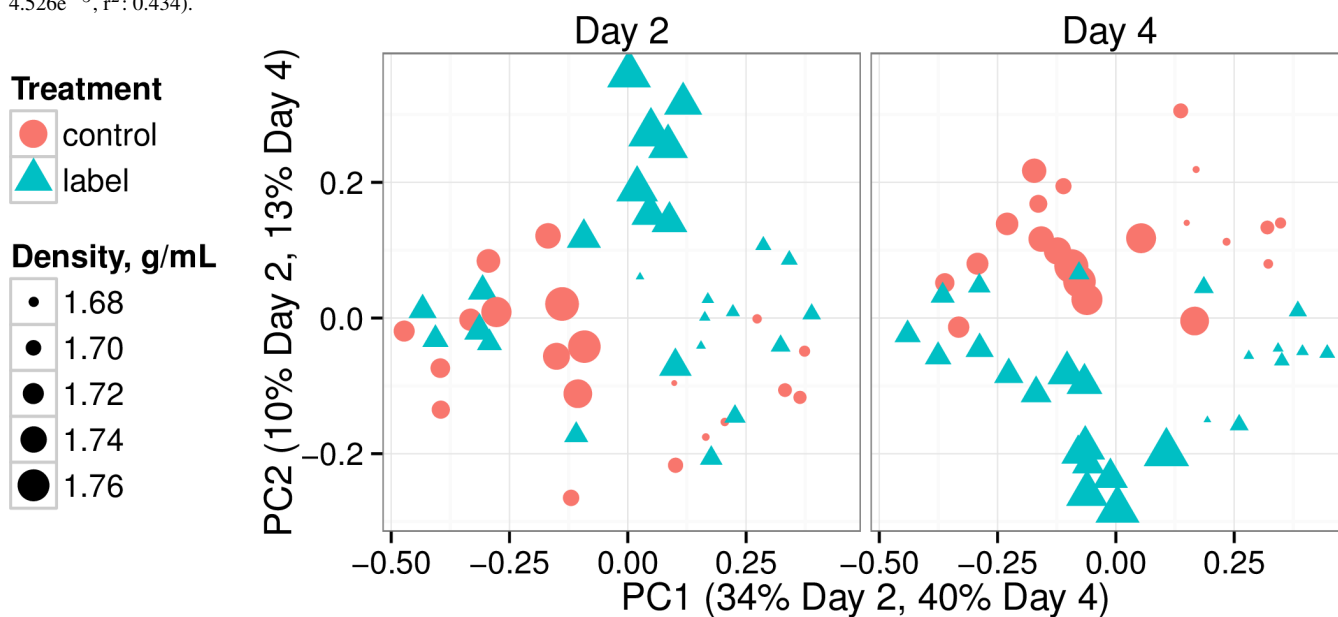
Figure S2. Distribution of sequences into top 9 phyla (phyla ranked by sum of all sequence annotations).
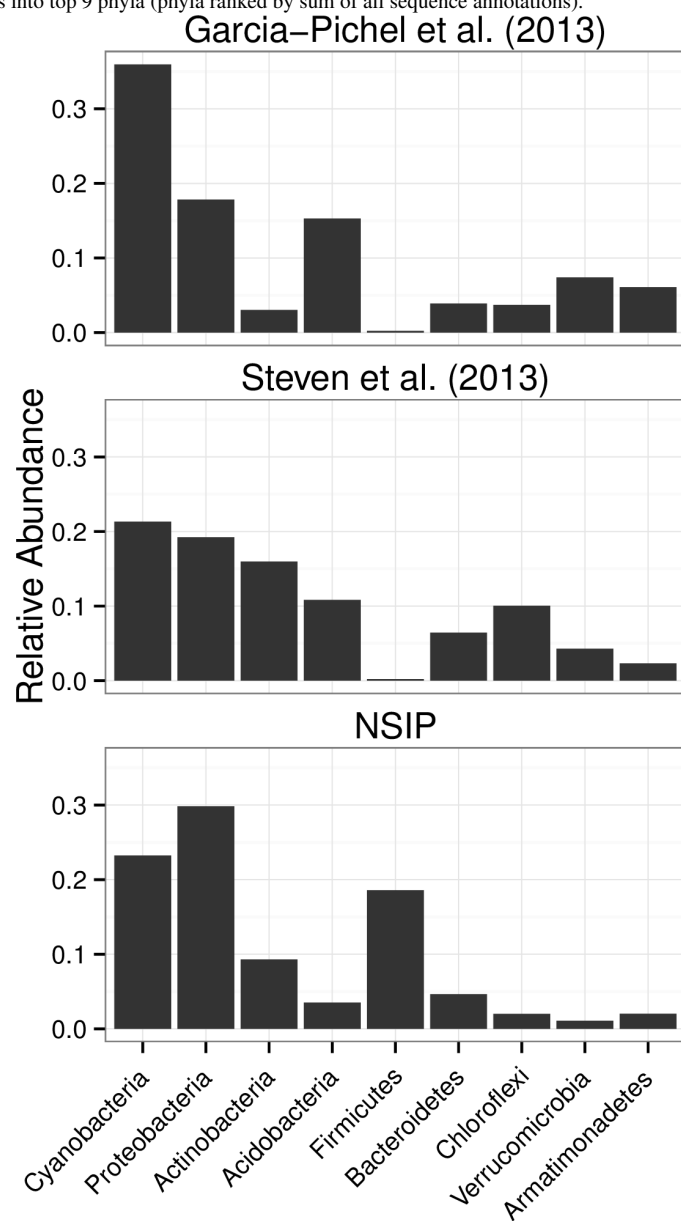
Figure S3. Relative abundance of selected heterocystous cyanobacterial OTUs with centroids from sequences described in Yeager et al. (2006) (see methods for selection criteria) in Steven et al. (2013) data set.

Figure S4. Rarefaction curves for all samples presented by Garcia-Pichel et al. (2013) and Steven et al. (2013). Inset is boxplot of estimated sampling effort for all samples in Garcia-Pichel et al. (2013) and Steven et al. (2013) (number of observed OTUs divided by number of CatchAll Bunge (2010) estimated total OTUs)

Figure S5. Counts of "responder" OTU occurrences in samples from Steven et al. (2013) and Garcia-Pichel et al. (2013). Steven et al. (2013) collected BSC samples (25 samples total) and samples from soil beneath BSC (17 samples total, "below" column in figure). Garcia-Pichel et al. (2013) collected samples from "dark" (9 samples total) and "light" (12 samples total) crusts in addition to "lichen" (2 samples total) dominated crusts.